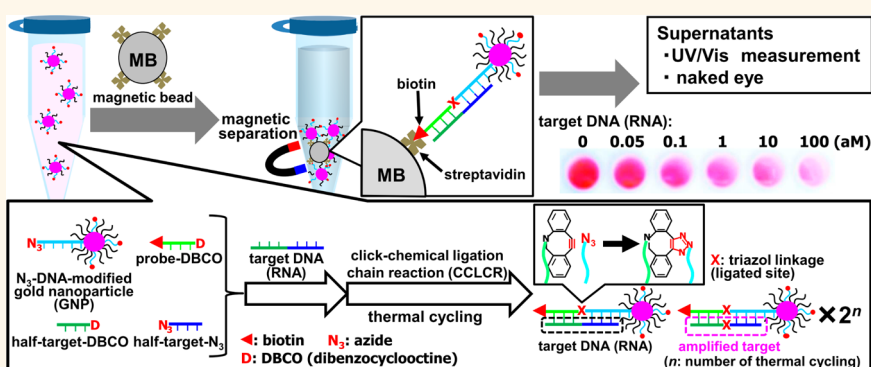


Ultrasensitive Detection of DNA and RNA Based on Enzyme-Free Click Chemical Ligation Chain Reaction on Dispersed Gold Nanoparticles

Daiki Kato and Motoi Oishi*

Division of Materials Science, Faculty of Pure and Applied Sciences, University of Tsukuba, 1-1-1 Tennoudai, Tsukuba, Ibaraki 305-8573, Japan

ABSTRACT



An ultrasensitive colorimetric DNA and RNA assay using a combination of enzyme-free click chemical ligation chain reaction (CCLCR) on dispersed gold nanoparticles (GNPs) and a magnetic separation process has been developed. The click chemical ligation between an azide-containing probe DNA-modified GNP and a dibenzocyclooctyne-containing probe biotinyl DNA occurred through hybridization with target DNA (RNA) to form the biotinyl-ligated GNPs (ligated products). Eventually, both the biotinyl-ligated GNPs and target DNA (RNA) were amplified exponentially using thermal cycling. After separation of the biotinyl-ligated GNPs using streptavidin-modified magnetic beads, the change in intensity of the surface plasmon band at 525 nm in the supernatants was observed by UV/vis measurement and was also evident visually. The CCLCR assay provides ultrasensitive detection (50 zM: several copies) of target DNA that is comparable to PCR-based approaches. Note that target RNA could also be detected with similar sensitivity without the need for reverse transcription to the corresponding cDNA. The amplification efficiency of the CCLCR assay was as high as 82% due to the pseudohomogeneous reaction behavior of CCLCR on dispersed GNPs. In addition, the CCLCR assay was able to discriminate differences in single-base mismatches and to specifically detect target DNA and target RNA from the cell lysate.

KEYWORDS: click chemistry · DNA · gold nanoparticles · ligation chain reaction · magnetic beads · RNA

Gold nanoparticles (GNPs) have received considerable interest because, when aggregated, there is a shift in the surface plasmon band (SPB) and a change in color from red to purple.^{1–4} On the basis of this principle, Mirkin's group was the first to use GNPs to detect target DNA.^{5–7} In these systems, dispersed DNA-modified GNPs were cross-linked to form aggregates through hybridization events with complementary target DNAs. As the aggregates accumulate, a significant red-to-purple color change can be easily visualized

by the naked eye. However, sensitivities of the cross-linked GNP-based colorimetric assays were only at nanomolar levels because a detectable shift of SPB and the change in color require the formation of large cross-linked GNPs.

Recently, a new class of cross-linked GNP-based system was developed utilizing the enzymatic ligation chain reaction (LCR) concept.^{8–10} Because this assay system is able to amplify both target DNA and cross-linked GNPs using thermal cycling, highly sensitive detection (attomolar levels) of target DNA

* Address correspondence to oishi@ims.tsukuba.ac.jp.

Received for review April 4, 2014 and accepted September 25, 2014.

Published online September 25, 2014
10.1021/nn503150w

© 2014 American Chemical Society

was achieved. Nevertheless, the cross-linked GNPs are unstable in solution, leading to time-dependent changes in SPB and color, and thus potentially inaccurate determinations of target DNA concentrations.^{11,12} Furthermore, the use of ligases for the cross-linked GNP-based LCR assay systems has several serious limitations, including the following: (i) There is steric hindrance of the DNA-modified GNPs, which results in a low amplification efficiency due to the low accessibility of ligases to the ligation site. (ii) As the number of thermal cycles increases, nonspecific aggregation of DNA-modified GNPs occurs because of the detachment of thiolated DNA from the GNPs, resulting from thiol exchange reactions with the dithiothreitol needed for enzymatic reactions. Thus, the number of thermal cycles has been limited to less than 30.^{8,9} (iii) Ligases have been reported to join DNA inefficiently on a target RNA,^{13–15} indicating that enzymatic LCR-based gene expression assays require cDNA synthesis using enzymatic reverse transcription of mRNA. Accordingly, a major key to the successful colorimetric detection of low levels of both DNA and RNA is the development of a non-cross-linked GNP-based assay system using an enzyme-free LCR.

Herein we describe a new non-cross-linked GNP-based assay system that is a combination of enzyme-free LCR on dispersed GNPs and a magnetic separation process using streptavidin-modified magnetic beads (MBs). This assay system relies on click chemical ligation between an azide-containing probe DNA immobilized on dispersed GNP (N₃-DNA-modified GNP) and a dibenzocyclooctyne (DBCO)-containing probe biotinyl DNA (probe-DBCO). This allows the dispersion of biotinyl-ligated GNPs (ligated products) during thermal cycling. Unlike conventional click chemistry with a copper catalyst, the click chemical ligation between DBCO-modified DNA and N₃-modified DNA proceeds spontaneously and smoothly in the presence of template DNA without any metal catalyst,¹⁶ even when immobilized on GNPs.¹⁷ In addition, both DBCO and N₃ groups are unreactive with various groups such as thiols, amines, and carboxylic acids. As a result, click chemical ligation between DBCO and N₃ groups avoids interference from coexisting biomolecules.^{18–20} Indeed, the click chemical ligation between DBCO-modified DNA and N₃-modified DNA could be applied to enzyme-free fluorescent-amplified aptasensors.²¹ Thus, this reaction is considered to be the best candidate for enzyme-free LCR-based DNA assay systems. The enzyme-free click chemical ligation chain reaction (CCLCR) assay system described in the current study exhibited exponential amplification of both the biotinyl-ligated GNPs and the target DNA (RNA). There was high amplification efficiency during thermal cycling but without the need for enzymatic reverse transcription of target RNA to the corresponding cDNA. A sensitivity of 50 zeptomolar (zM = 10^{−21} M: several

copies in 70 μ L sample) was achieved for target DNA (RNA), as well as very high discrimination of single-base mismatches.

RESULTS AND DISCUSSION

Design Principles of the Assay Systems. Our strategy for developing a new assay system for detecting DNA (RNA) was based on a combination of magnetic separation and enzyme-free click chemical ligation on dispersed GNPs (Figure 1). The current study reports on proof-of-concept experiments. A DNA sequence associated with the hepatitis A virus Vall7 polyprotein gene (HAV) was chosen as the target DNA. A target RNA sequence identical to that of the target DNA was used for comparison purpose. The DNA and RNA sequences used in this study are listed in Table S1. Unlike cross-linked GNP-based systems, the current system does not require the formation of large assemblies of the biotinyl-ligated GNPs and MBs to detect target DNA (RNA). Therefore, the GNPs (average diameter of 15 nm, Figure S1) were modified using two types of dithiolated-DNAs with the same length (20 nucleotides). One was a probe-N₃ with a half complementary sequence to the target DNA. The other was a diluent strand (T₂₀) to reduce formation of large assemblies of the biotinyl-ligated GNPs and MBs as well as the waste of probe-DBCO, because one or a few biotin molecules on the GNP are sufficient for the formation of assemblies of the biotinyl-ligated GNPs and MBs. The feed ratio of probe-N₃ and the diluent strand was 1:8. The average total number of DNA strands per particle was 121 \pm 2 strands/particle by using literature methods.^{22–25} Since both the probe-N₃ and diluent strand are the same length, the numbers of probe-N₃ and diluent strands per particle based on the feed ratio were assumed to be 13 strands/particle and 108 strands/particle, respectively. Three methods, including a nonamplification assay (Figure 1a), an asymmetric CCLCR assay (linear amplification; Figure 1b), and a CCLCR assay (exponential amplification; Figure 1c), were used to detect target DNA. In the case of the nonamplification assay, a mixture of target DNA, N₃-DNA-modified GNPs ([GNP] = 1.15 nM and [probe-N₃] = 15 nM), and probe-DBCO (15 nM) was incubated in phosphate buffer (PB) (10 mM; pH 7.0 containing 0.1 M NaCl) at room temperature for 15 min to ligate between probe-DBCO and N₃-DNA-modified GNP through hybridization with the target DNA. For the asymmetric CCLCR and CCLCR assays, mixtures of the N₃-modified GNP, probe-DBCO, and target DNA, in the absence (asymmetric CCLCR assay) or presence (CCLCR assay) of a pair of half-target-N₃ (15 nM) and half-target-DBCO (15 nM), were thermal cycled (one cycle involved denaturation at 85 °C for 30 s and hybridization/ligation at 25 °C for 150 s). During thermal cycling, the asymmetric CCLCR assay linearly amplified only the biotinyl-ligated GNP, whereas the CCLCR assay

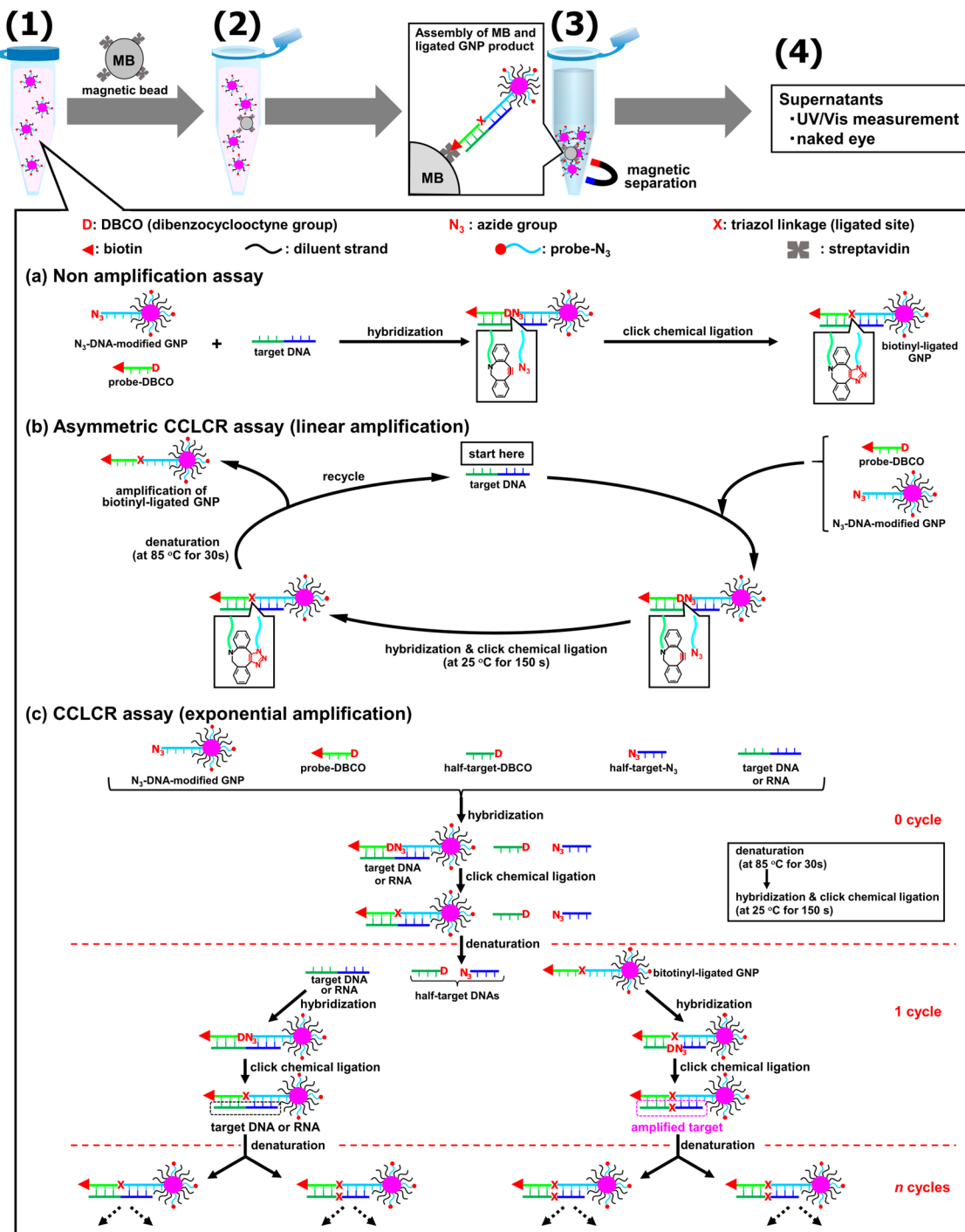


Figure 1. Schematic illustration of the principles of DNA (RNA) detection: (1) (a) nonamplification assay, (b) asymmetric CCLCR assay (linear amplification), and (c) CCLCR assay (exponential amplification) → (2) addition of MBs → (3) magnetic separation of the biotinyl-ligated GNP → (4) detection of target DNA (RNA) from the supernatant. (a) Nonamplification assay: a mixture of N₃-DNA-modified GNPs, probe-DBCO, and target DNA was incubated at room temperature for 15 min to ligate between probe-DBCO and N₃-DNA-modified GNP through hybridization with the target DNA. (b) Asymmetric CCLCR assay: a mixture of the N₃-modified GNP, probe-DBCO, and target DNA was thermal cycled to amplify linearly the biotinyl-ligated GNP. (c) CCLCR assay: a mixture of the N₃-modified GNP, probe-DBCO, target DNA, and a pair of half-target-N₃ and half-target-DBCO were thermal cycled to amplify exponentially both the biotinyl-ligated GNP and the target DNA (RNA).

exponentially amplified both the biotinyl-ligated GNP and the target DNA (RNA).

MBs were then added to the solutions resulting from the nonamplification, asymmetric, and CCLCR assays. Each solution was incubated at room

temperature for 30 min to form assemblies of the biotinyl-ligated GNPs and MBs. The assemblies, along with unattached MBs, were pulled to the wall of the reaction tube by a magnetic field. Changes in the SPB and the color of the supernatants were observed by

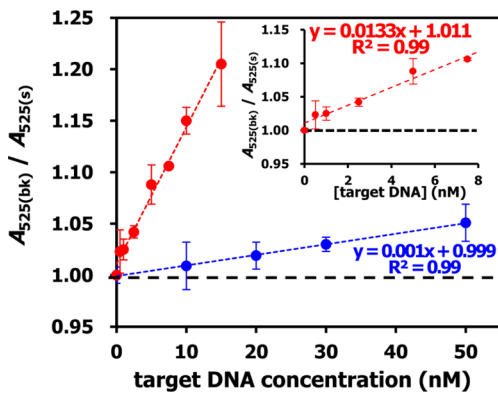


Figure 2. $A_{525(\text{bk})}/A_{525(\text{s})}$ ratios for the nonamplification (blue circles) and asymmetric CCLCR assays using 40 thermal cycles (red circles) at different target DNA concentrations. The inset shows the response to 0–7.5 nM target DNA in the asymmetric CCLCR assay. Mean values and standard deviations were obtained from three independent experiments.

UV/vis measurement and the naked eye, respectively. In these systems, we only need to focus on the change in absorbance of SPB at 525 nm (A_{525}) rather than the complicated spectra of cross-linked GNPs because of the stability of the dispersed biotinyl-ligated GNPs resulting in minimal time-dependent changes in SPB (color), allowing simple detection of target DNA and target RNA.

Detection of DNA by the Nonamplification and Asymmetric CCLCR Assays. Target DNA was initially detected using a nonamplification assay that was similar to previously reported cross-linked GNP-based systems.^{5–7} As the concentration of target DNA increased, the ratio ($A_{525(\text{bk})}/A_{525(\text{s})}$) of the blank ($A_{525(\text{bk})}$) and the sample ($A_{525(\text{s})}$) increased (Figure 2, blue circles). The $A_{525(\text{bk})}/A_{525(\text{s})}$ showed a good linear relationship for target DNA concentration. The limit of detection (LOD), calculated as 3 times the standard deviation (σ) of $A_{525(\text{bk})}$, was 24 nM. The nanomolar level of this LOD was comparable to those reported for other cross-linked GNP-based systems.^{26,5–7}

The asymmetric CCLCR assay linearly amplifies biotinyl-ligated GNPs through hybridization, click chemical ligation, and denaturation processes using thermal cycling. As shown in Figure S2a, a linear increase in the $A_{525(\text{bk})}/A_{525(\text{s})}$ was observed with an increasing number of thermal cycles at different target DNA concentrations. In addition, the slopes of each fit line in Figure S2a linearly increased with increasing target DNA concentrations (Figure S2b). These facts strongly suggest that the biotinyl-ligated GNPs (ligated products) were amplified linearly by the thermal cycling process through click chemical ligation between the probe-DBCO and the N_3 -DNA-modified GNPs in the presence of target DNA. The asymmetric assay, after 40 thermal cycles, had a 35-fold lower LOD (0.68 nM) compared to that of the nonamplification assay (Figure 2, red circles).

However, this detection limit is insufficient to detect target DNA from biological samples.

Detection of DNA and RNA by the CCLCR Assay. To further improve the detection sensitivity, a CCLCR assay system was constructed by adding a pair of half-target- N_3 and half-target-DBCO to a mixture containing the N_3 -modified GNPs, probe-DBCO, and target DNA. Ideally, the CCLCR assay should enable amplification of both the biotinyl-ligated GNPs and the target DNA (RNA) by 2^n -fold, with n being the number of thermal cycles.²⁷ Indeed, as the number of thermal cycles increased, there was an exponential increase in the $A_{525(\text{bk})}/A_{525(\text{s})}$ at different target DNA concentrations (Figure 3a). As seen in Figure S3, the UV/vis spectrum ($\lambda_{\text{max}} = 522 \text{ nm}$) of the supernatant after 40 thermal cycles in the presence of 100 aM target DNA is identical to that of as-prepared N_3 -modified GNPs ($\lambda_{\text{max}} = 522 \text{ nm}$) except for absorbance intensity. Thus, peak shifts due to the non-cross-linking aggregation of GNPs or the change of surface property were little observed, indicating that the increase in the $A_{525(\text{bk})}/A_{525(\text{s})}$ is indeed caused by the removal of the biotinyl-ligated GNPs using MBs. In the absence of target DNA, a decrease in $A_{525(\text{bk})}$ was not observed even after 40 thermal cycles (Figure S3), indicating that nonspecific click chemical ligation between free N_3 and DBCO groups did not occur under these thermal cycling conditions. Nevertheless, the $A_{525(\text{bk})}/A_{525(\text{s})}$ plateaued gradually after 30 thermal cycles at higher target DNA concentrations (1 and 10 fM) probably due to depletion of the probe and half-target DNAs. The number of thermal cycles needed to reach an $A_{525(\text{bk})}/A_{525(\text{s})}$ of 1.07 (the C_t value) was also linearly dependent on the log-concentration of target DNA (Figure 3b), strongly indicating that thermal cycling exponentially amplified both the biotinyl-ligated GNPs and the target DNA. The slope (-3.82 , $C_t/\log[\text{target DNA}]$) of the fit line in Figure 3b and the equation $E = 10^{-1/\text{slope}} - 1$ were used to calculate an amplification efficiency (E) of 83%. In contrast to an E of only 55% seen with enzymatic LCR between DNA-modified GNPs,²⁸ this high E most likely results from a facilitation of the hybridization of target DNA and ligation reaction in an enzyme-free CCLCR on dispersed GNPs, allowing a nearly homogeneous reaction behavior.

As the concentration of target DNA increased after 40 thermal cycles, the color of the supernatants changed from deep red to light red (or pink), which could be visualized by the naked eye (Figure 3c inset). Recently, Pompa *et al.* reported that the color of the assemblies of GNPs (40 nm) and MBs changed also from yellowish-brown (MB) to reddish-brown (assembly) to detect target DNA easily by the naked eye.²⁹ Unfortunately, this color change was hardly observed in the CCLCR system presumably due to the small size (15 nm) of the GNP and/or insufficient formation of the assemblies. Eventually, the CCLCR assay had a significant low LOD

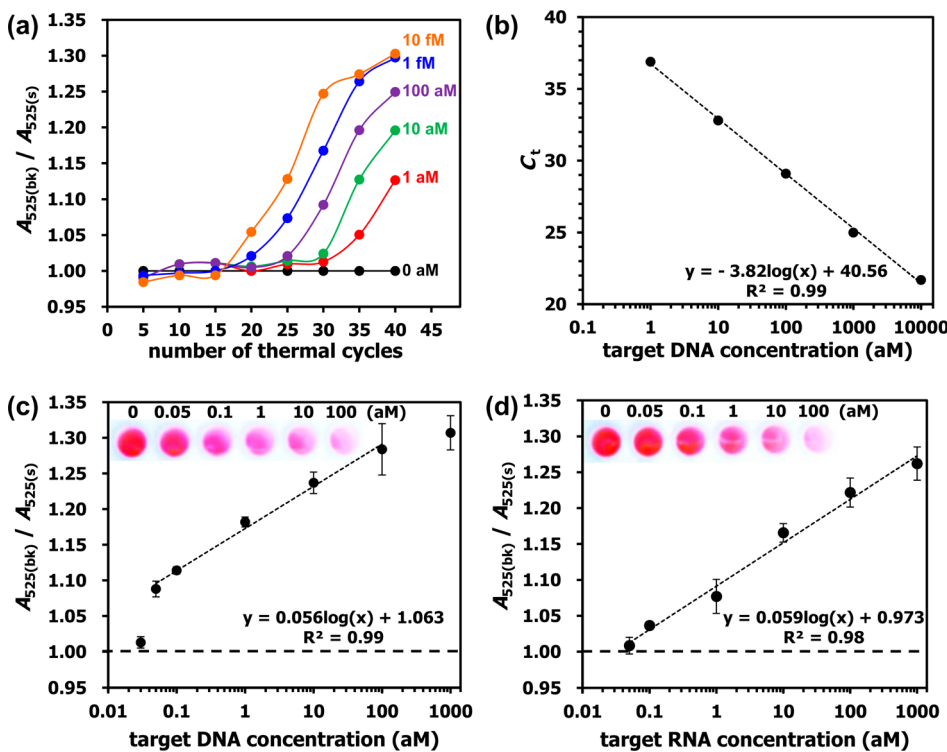


Figure 3. (a) $A_{525(\text{bk})}/A_{525(\text{s})}$ ratios for the CCLCR assay as a function of the number of thermal cycles and the target DNA concentrations (from left to right, 10 fM, 1 fM, 100 aM, 10 aM, 1 aM, and 0 aM). (b) The corresponding calibration curve of target DNA concentration vs C_t (number of thermal cycles required to reach an $A_{525(\text{bk})}/A_{525(\text{s})}$ of 1.07). (c) $A_{525(\text{bk})}/A_{525(\text{s})}$ ratios at different target DNA concentrations using 40 thermal cycles. The inset shows a photograph of the supernatants at different target DNA concentrations. (d) $A_{525(\text{bk})}/A_{525(\text{s})}$ ratios at different target RNA concentrations using 40 thermal cycles. The inset shows a photograph of the supernatants at different target RNA concentrations. Mean values and standard deviations were obtained from three independent experiments.

(50 zM) (Figure 3c) that was several orders of magnitude lower compared to those reported for other cross-linked GNP-based enzymatic LCR systems (1.5–20 aM).^{8–10} This ultralow LOD of the CCLCR assay is likely due to (i) high amplification efficiency caused by the nearly homogeneous reaction behavior of the enzyme-free CCLCR on dispersed GNPs and (ii) no limit to the number of thermal cycles because of the absence of detachment of thiol-DNAs from the GNPs through a thiol exchange reaction with dithiothreitol. Notably, the 70 μL sample volume (50 zM) used in this experiment contained approximately three target DNA strands, showing that the CCLCR assay provides a sensitivity comparable to that of PCR-based techniques.^{30–32} Moreover, the CCLCR assay showed a dynamic range over 3 orders of magnitude of target DNA concentrations. It should be noted that the CCLCR assay also detects target RNA (mock mRNA) (Figures 3d and S4). The LOD (50 zM, 3 target RNA strands) and E (82%) for target RNA were similar to those for the detection of target DNA. In contrast to enzymatic LCR cross-linked GNP-based systems, the CCLCR assay can directly detect target mRNAs without prior reverse transcription to the corresponding cDNA. Although further optimization of assay conditions including thermal cycling conditions (hybridization/ligation time) and concentration of probe- and half-target DNAs is

required to improve low $A_{525(\text{bk})}/A_{525(\text{s})}$ (insufficient formation of the assemblies) presumably caused by low ligation efficacy, the relative standard deviation (RSD %) of all plots in Figure 3c and d is less than 3%. Thus, the current CCLCR assay without optimization showed low LOD (50 zM) with high reproducibility.

To confirm whether the increases in the $A_{525(\text{bk})}/A_{525(\text{s})}$ seen during the CCLCR assay resulted from click chemical ligation, a control experiment was carried out using a biotin-containing probe DNA without the DBCO group (probe-DNA-biotin) instead of the probe-DBCO in the presence of N_3 -DNA-modified GNPs, a pair of half-target- N_3 and half-target-DBCO, and target DNA (100 aM). The resulting $A_{525(\text{bk})}/A_{525(\text{s})}$ was as low as 1.0 (Figure S5), indicating that there was no amplification of either the biotinyl-ligated GNP or the target DNA. Thus, click chemical ligation between N_3 -DNA-modified GNP and the probe-DBCO is a key step for the CCLCR assay.

Additional evidence for the occurrence of click chemical ligation was obtained by measuring the A_{525} of the supernatants from two types of assemblies of MBs and GNPs: one that was prepared using the CCLCR assay in the presence of target DNA (ligation-related assemblies) and the other that was prepared using the probe-DNA-biotin instead of the probe-DBCO in the presence of target DNA (non-ligation-related assemblies).

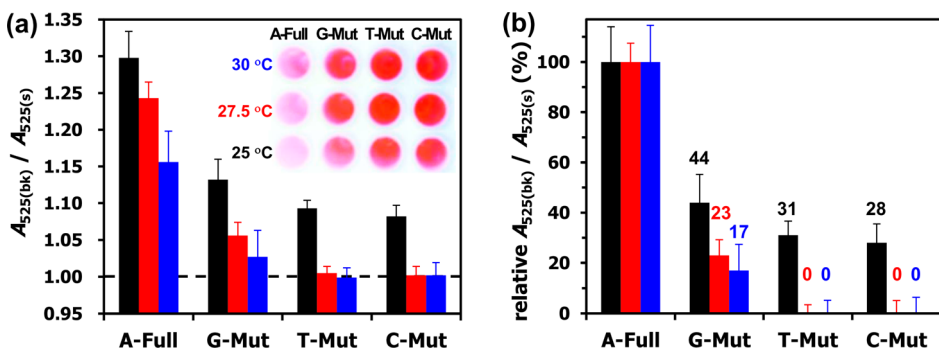


Figure 4. Selectivity of the CCLCR assay using 40 thermal cycles at different hybridization/ligation temperatures (25 °C black bars, 27.5 °C red bars, and 30 °C blue bars) when analyzing the full-match target DNA (A-Full) and single-base mismatch target DNAs (T-Mut, C-Mut, and G-Mut) at 100 aM. (a) $A_{525(bk)}/A_{525(s)}$ ratios for A-Full, T-Mut, C-Mut, and G-Mut after 40 thermal cycles. The inset shows a photograph of the supernatants. (b) Relative $A_{525(bk)}/A_{525(s)}$ ratios for A-Full, T-Mut, C-Mut, and G-Mut after 40 thermal cycles, where $A_{525(bk)}/A_{525(s)}$ induced by A-Full is 100%, while $A_{525(bk)}/A_{525(s)}$ for the blank is 0%. Mean values and standard deviations were obtained from three independent experiments.

Both assemblies were collected by magnetic separation to remove free N_3 -DNA-modified GNPs. The resulting assemblies were dispersed in PB and then separated magnetically at 25 or 80 °C. The supernatants were measured by UV/vis spectroscopy. After magnetic separation at 25 °C, the supernatants from both the non-ligation-related assemblies (Figure S6a) and the ligation-related assemblies (Figure S6b) showed no A_{525} . When magnetic separation of non-ligation-related assemblies was carried out at 80 °C, thereby denaturing the N_3 -DNA-modified GNP/target DNA/probe-DNA-biotin duplex, an increase in A_{525} was observed due to redispersion of GNPs into the solution (Figure S6a). In sharp contrast, there was little change in A_{525} of the supernatant from the ligation-related assemblies even after magnetic separation at 80 °C (Figure S6b). This suggests that the ligation-related assemblies were thermally irreversible by formation of a covalent linkage (X: triazol linkage) between N_3 -DNA-modified GNPs and the probe-DBCO through click chemical ligation. These facts strongly indicate that click chemical ligation between the N_3 -DNA-modified GNPs and the probe-DBCO occurred during the CCLCR assay.

Discrimination of Single-Base Mismatches. The CCLCR assay has been used to assess single-base mismatches as a model of single-nucleotide polymorphisms (SNPs),^{33,34} which are important in gene expression. Single-base mismatch target DNAs including T (T-Mut), C (C-Mut), and G (G-Mut) were compared to fully complementary target DNA (A-Full) (Table S1). A series of target DNA sequences with a single-base mismatch at the fourth position from the ligation site were selected, because the difference in melting temperature (T_m) between full-match and mismatches is considered to be sufficient for the mismatch discrimination. Initially, all other conditions, including the number of thermal cycles (40 cycles), target DNA concentration (100 aM), and thermal cycling conditions (denaturation at 85 °C for 30 s and hybridization/ligation at 25 °C for 150 s), were identical to those

described for the CCLCR assay. Note that only A-Full showed a significant increase in the $A_{525(bk)}/A_{525(s)}$, whereas the $A_{525(bk)}/A_{525(s)}$ for T-Mut and C-Mut increased a little (Figure 4a, black bars). The G-Mut showed some increase in the $A_{525(bk)}/A_{525(s)}$, possibly because the T/G pair (wobble base pair) is known to minimize mismatched instability.³⁵

As the temperature of the hybridization/ligation process increased from 25 °C to 27.5 or 30 °C (Figure 4a, red and blue bars), there was a significant decrease in the $A_{525(bk)}/A_{525(s)}$ for single-base mismatch target DNAs, although the $A_{525(bk)}/A_{525(s)}$ of A-Full only decreased slightly. The difference in the color of the supernatants between full match and mismatches could also be visualized by the naked eye (Figure 4a inset). Figure 4b shows the relative $A_{525(bk)}/A_{525(s)}$ response to single-base mismatch target DNAs, assuming that the $A_{525(bk)}/A_{525(s)}$ induced by A-Full is 100%, while the $A_{525(bk)}/A_{525(s)}$ for the blank is 0%. Note that the relative $A_{525(bk)}/A_{525(s)}$ responses to G-Mut, T-Mut, and C-Mut at 30 °C were 17%, 0%, and 0%, respectively, demonstrating high discrimination of single-base mismatches. This is most likely because the probe- N_3 on GNPs is not perfectly complementary to the single-base mismatch target DNAs, leading to a decrease in the T_m 's of duplexes composed of the probe- N_3 and single-base mismatch target DNAs (Table S1). Thus, click chemical ligation between N_3 -DNA-modified GNPs and the probe-DBCO occurred inefficiently. These facts clearly demonstrate that single-base mismatch DNAs could be distinguished easily by changing the temperature of the hybridization/ligation process.

Detection of DNA in the Presence of Genomic DNA. To evaluate the effect of the genomic DNA matrix on the detection of target DNA (1 aM), the CCLCR assay was carried out in the presence of a large excess of genomic DNA. Salmon sperm DNA was used to imitate a complicated matrix because of its large complex DNA sequences. Weight ratios of target DNA to genomic

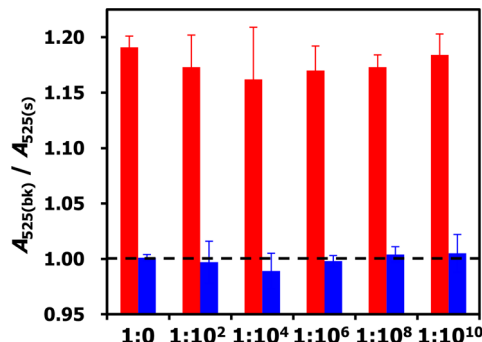


Figure 5. $A_{525(\text{bk})}/A_{525(\text{s})}$ ratios for CCLCR assay after 40 thermal cycles with 1 aM (red bars) or 0 aM (blue bars) target DNA in the presence of increasing amounts of genomic DNA (target DNA/genomic DNA weight ratios were 1:0 to 1:10¹⁰). Mean values and standard deviations were obtained from three independent experiments.

DNA varying from 1:0 to 1:10¹⁰ were used. As shown in Figure 5, there was no change in the $A_{525(\text{bk})}/A_{525(\text{s})}$ caused by target DNA even at target DNA/genomic DNA weight ratios up to 1:10¹⁰. Thus, satisfactory recovery (99%) for the detection of target DNA (1 aM corresponds to 42 target DNA strands) in the genomic DNA (1:10¹⁰) was observed. This indicates that genomic DNA does not interfere with this assay. Assuming that a single cell contains one target DNA strand, 42 target DNA strands correspond to 42 cells. Since the total mass of genomic DNA in a single human cell is approximately 7 pg/cell,³⁶ the target DNA to genomic DNA ratio in a single human cell is assumed to be 1 (target DNA strand):7 (pg). This ratio is less than the target DNA/genomic DNA weight ratio of 1:10⁸ corresponding to 1 (target DNA strand):17 (pg). Thus, the CCLCR assay is highly selective toward the target DNA in the presence of a large excess of genomic DNA.

Detection of DNA and RNA from Cell Lysate. To test the feasibility of more practical application of the CCLCR system, we further conducted its detection of target DNA (1 aM corresponds to 42 target DNA strands) and target RNA (1 aM corresponds to 42 target RNA strands) from human cell lysate, because human cell lysate is realistically complex matrixes containing a variety of proteins, genomic DNA, total RNA, and other contaminants. As shown in Table 1, the buffer system and cell lysate system have comparable $A_{525(\text{bk})}/A_{525(\text{s})}$ with high reproducibility; thus satisfactory recovery (%) and RSD % for the detection of both target DNA and target RNA in the presence of cell lysate were 99–105% and <1.0%, respectively. Assuming that a single cell contains one target DNA (RNA) strand, 42 target DNA (RNA) strands correspond to 42 cells. The total

TABLE 1. Detection of DNA and RNA from Buffer and Cell Lysate

| sample | buffer system $A_{525(\text{bk})}/A_{525(\text{s})}^a$ | cell lysate system $A_{525(\text{bk})}/A_{525(\text{s})}^a$ | recovery (%) |
|-------------------|---|--|--------------|
| target DNA (1 aM) | 1.19 ± 0.01 | 1.25 ± 0.01 | 105 |
| target RNA (1 aM) | 1.07 ± 0.03 | 1.06 ± 0.01 | 99 |

^a Mean values and standard deviations were obtained from three independent experiments.

mass of proteins in a single human cell is known to be approximately 200–400 pg/cell.³⁷ Thus, the 70 μL sample volume used in this experiment contained approximately 1.5 μg of protein, which is more than the total mass of proteins (16.8 ng) of 42 cells. This fact indicates that target mRNA will be detected directly from cell lysate without the need for enzymatic reverse transcription of target mRNA to the corresponding cDNA. The CCLCR assay will allow easy elimination of interference from coexisting biological molecules in a real sample.

CONCLUSIONS

The current study describes an ultrasensitive colorimetric assay for DNA and RNA that utilizes enzyme-free CCLCR on dispersed GNPs and magnetic separation of the biotinyl-ligated GNPs using MBs. Enzyme-free click chemical ligation between N₃-DNA-modified GNP and a probe-DBCO occurred during thermal cycling in the presence of target DNA (RNA) to form the biotinyl-ligated GNPs. This is a key step for the exponential amplification of both the biotinyl-ligated GNPs and the target DNA (RNA). After magnetic separation of the biotinyl-ligated GNPs, simple measurement of A_{525} of the supernatants, rather than analyzing complicated spectra of cross-linked GNPs, is all that is necessary. Thus, the CCLCR assay system provides simplicity as well as ultrasensitive detection (50 zM corresponds to several copies) for both target DNA and target RNA (mock mRNA target). Unlike enzymatic LCR between DNA-modified GNPs, high amplification efficiency (82%) was attained due to the pseudohomogeneous reaction behavior of CCLCR on dispersed GNPs. In addition, the CCLCR assay was able to discriminate single-base mismatch DNAs by changing the thermal cycling conditions and allowed easy elimination of interference from complex biological matrixes. Therefore, this is a simple, ultrasensitive, selective, and effective assay system that has enormous potential for the detection of DNA, SNPs, and RNAs, possibly including micro-RNAs.

METHODS

Chemicals and Instruments. Citrate-coated 15 nm gold nanoparticle solution (BBI solution, USA), sodium chloride (NaCl: Wako,

Japan), phosphate buffer powder-pH 7.0 (PB: Wako, Japan), DNA from salmon sperm (Wako, Japan), 2-mercaptopethanol (Sigma-Aldrich, USA), MagnosphereM300/streptavidin (MB: JSR

Life Sciences, Japan), Mg-ion chelate resin (InstaGene matrix: BIO-RAD, USA), and RNasin Plus ribonuclease inhibitor (Promega, USA) were used without further purification. Water was purified using the Milli-Q system (Millipore, USA). Oligonucleotides were purchased from Tsukuba Oligo Service, Co., Japan, and the DNA and RNA sequences employed are shown in Table S1. A sequence of target DNA is associated with the hepatitis A virus Val7 polyprotein gene: AF396407, 2457bp, N700–729 (HAV). Centrifugation of gold nanoparticle solutions was carried out using Micro refrigerated centrifuge model 3740 (Kubota, Japan). UV/vis and fluorescence spectra were recorded using a UV-2550 spectrometer (Shimadzu, Japan) and F-7000 spectrometer (Hitachi, Japan), respectively. Thermal cycling was performed in an MJ Mini PCR (Bio-Rad, USA). Dynamic light scattering (DLS) measurement was carried out at 25 °C using Zetasizer Nano-ZS (Malvern, U.K.) equipped with a 4.0 mW He–Ne laser ($\lambda = 633$ nm).

Preparation of N₃-DNA-Modified GNP. N₃-DNA-modified GNPs were prepared according to the literature.^{22–25} A citrate-coated 15 nm GNP solution (250 μ L, 2.3 nM, 1.4×10^{12} particles/mL) was added to a mixture of diluent strand (16 μ L, 25 μ M) and probe-N₃ (2 μ L, 25 μ M) in water (final concentrations were as follows: [GNP] = 2.15 nM; [diluent strand] = 1.5 μ M; and [probe-N₃] = 0.187 μ M). The resulting mixture was incubated at room temperature for 2 h. PB (100 mM; pH 7.0 containing 1 M NaCl) was added stepwise to bring the total NaCl concentration to 200 mM. After standing for 16 h, the final mixture was aged for 24 h and then centrifuged three times at 20000g for 30 min with 250 μ L of PB (10 mM; pH 7.0 containing 0.1 M NaCl) to remove free DNA. The supernatant was removed, and the red oily precipitate was dispersed in 100 μ L of PB (10 mM; pH 7.0 containing 0.1 M NaCl) to a final GNP concentration of 4.6 nM ([probe-N₃] = 60 nM). The average diameter of the N₃-DNA-modified GNPs was 31 nm as measured by DLS (Figure S1). Approximately 20% of the original concentration of GNPs was lost during preparation.

Quantitation of Immobilized DNA Strands on GNPs. The quantitation of immobilized DNA strands on GNPs was carried out according to the literature.^{22–25} Fluorescein isothiocyanate (FITC)-labeled DNA (FITC-DNA) with 20 nucleotides (T₂₀) was used in place of probe-N₃ and diluent strand to quantify the amount of immobilized DNA strands on the GNPs. Procedures for the preparation of FITC-DNA-modified GNPs were identical to those described for the preparation of N₃-DNA-modified GNPs. A 100 μ L amount of 143 mM 2-mercaptoethanol in PB (10 mM; pH 7.0 containing 0.1 M NaCl) was added to the FITC-DNA-modified GNP solution to bring the final concentration of 2-mercaptoethanol to 35.8 mM. After shaking for 24 h at room temperature, the solutions containing displaced DNAs were separated from the GNP aggregates by centrifugation at 20000g for 30 min. Aliquots of the supernatant were measured by fluorescence spectroscopy. Fluorescence maximums (measured at 516 nm) were converted to molar concentrations of FITC-DNA by interpolation from a standard linear calibration curve prepared with known concentrations of FITC-DNAs using identical buffer pH, salt, and 2-mercaptoethanol concentrations. The average number of DNA strands per particle (121 \pm 2 strands/particle) was obtained by dividing the measured DNA molar concentration by the GNP concentration.

Detection of DNA by a Nonamplification Assay. The detection of DNA using a nonamplification assay was carried out in PB (10 mM; pH 7.0 containing 0.1 M NaCl) in a total volume of 69 μ L. The assay mixture consisted of 17.5 μ L of N₃-DNA-modified GNP ([GNP] = 4.6 nM and [probe-N₃] = 60 nM in 10 mM PB), 7 μ L of probe-DBCO (150 nM in 10 mM PB), and 7 μ L of various concentrations of target DNA in 10 mM PB. Final concentrations of GNP, probe-N₃, probe-DBCO, and target DNAs were 1.15, 15, 15, and 10–50 nM, respectively. The mixture was stirred gently at room temperature for 15 min to allow the GNPs to hybridize and ligate. MBs (1 μ L, 10 mg/mL, 6×10^8 beads/mL) were then added to the mixture and allowed to form assemblies of MBs with the biotinyl-ligated GNPs (ligated products) using gentle mixing at room temperature for 30 min. The final volume of the system was 70 μ L. The assemblies, along with unattached MBs, were pulled to the wall of the reaction tube over several minutes by applying a magnetic field. Finally,

A_{525} of the supernatant was measured by UV/vis spectroscopy with a 50 μ L quartz microcuvette.

Detection of DNA by Asymmetric CCLCR Assay. The asymmetric CCLCR assay was carried out in PB (10 mM; pH 7.0 containing 0.1 M NaCl) in a total volume of 69 μ L. The assay mixture consisted of 17.5 μ L of N₃-DNA-modified GNPs ([GNP] = 4.6 nM and [probe-N₃] = 60 nM in 10 mM PB), 7 μ L of probe-DBCO (150 nM in 10 mM PB), and 7 μ L of various concentrations of target DNA in 10 mM PB. Final concentrations of GNP, probe-N₃, probe-DBCO, and target DNAs were 1.15, 15, 15, and 0.05–15 nM, respectively. The mixture was stirred gently at room temperature for 15 min. Reactions were performed under the following thermal cycling conditions (denaturation at 85 °C for 30 s and hybridization/ligation at 25 °C for 150 s) using a thermal cycler designed for PCR. After a designated number of thermal cycles, MBs (1 μ L, 10 mg/mL, 6×10^8 beads/mL) were added to the mixture and allowed to form assemblies of MBs with the biotinyl-ligated GNPs with gentle mixing at room temperature for 30 min. The final volume of the system was 70 μ L. The assemblies, along with unattached MBs, were pulled to the wall of the reaction tube over several minutes by applying a magnetic field. Finally, A_{525} of the supernatant was measured by UV/vis spectroscopy with a 50 μ L quartz microcuvette.

Detection of DNA and RNA by the CCLCR Assay. The CCLCR assay was carried out in PB (10 mM; pH 7.0 containing 0.1 M NaCl) in a total volume of 69 μ L. The assay mixture consisted of 17.5 μ L of N₃-DNA-modified GNPs ([GNP] = 4.6 nM and [probe-N₃] = 60 nM in 10 mM PB), 7 μ L of probe-DBCO (150 nM in 10 mM PB), 7 μ L of half-target-N₃ (150 nM in 10 mM PB), 7 μ L of half-target-DBCO (150 nM in 10 mM PB), and 7 μ L of various concentrations of target DNA or target RNA in 10 mM PB. Final concentrations of GNPs, probe-N₃, probe-DBCO, half-target-N₃, half-target-DBCO, and target DNA were 1.15 nM, 15 nM, 15 nM, 15 nM, 15 nM, and 10 zM to 10 fM, respectively. The mixture was stirred gently at room temperature for 15 min. Reactions were performed under the same conditions as the asymmetric CCLCR assay using a thermal cycler designed for PCR. After a designated number of thermal cycles, the MBs (1 μ L, 10 mg/mL, 6×10^8 beads/mL) were added to the mixture and allowed to form assemblies of MBs with the biotinyl-ligated GNPs with gentle mixing at room temperature for 30 min. The final volume of the system was 70 μ L. The assemblies, along with unattached MBs, were pulled to the wall of the reaction tube over several minutes by applying a magnetic field. Finally, A_{525} of the supernatant was measured by UV/vis spectroscopy with a 50 μ L quartz microcuvette.

Discrimination of Single-Base Mismatches. DNAs with single-base mutations including T (T-Mut), C (C-Mut), and G (G-Mut) were used to assess the ability of the CCLCR assay to differentiate between single-base mismatch DNAs and target DNA (A-Full). Except for the thermal cycling conditions (denaturation at 85 °C for 30 s and hybridization/ligation at 25, 27.5, or 30 °C for 150 s), the other assay conditions, including the number of thermal cycles (40), single-base mismatch target DNA concentration (100 aM), and the detection procedures, were identical to those for the CCLCR assay.

Detection of DNA in the Presence of Genomic DNA. The CCLCR assay was carried out in the presence of a large excess of genomic DNA. Target DNA/genomic DNA weight ratios were varied from 1:0 to 1:10¹⁰. The concentration of target DNA was 1 aM, and the number of thermal cycles was 40. Thermal cycling conditions (denaturation at 85 °C for 30 s and hybridization/ligation at 25 °C for 150 s) and the detection procedures were identical to those described previously for the CCLCR assay.

Detection of DNA and RNA from Cell Lysate. Human cell lysate was prepared from oral mucosa cells of one healthy volunteer in our laboratory. Oral mucosa cells were collected through vigorous rinsing of the mouth using saline (2 mL). The cell suspension was centrifuged at 5600g for 2 min, then washed with 500 μ L of PB (10 mM; pH 7.0 containing 0.1 M NaCl) three times. The cell pellet was dispersed in 40 μ L of PB (10 mM; pH 7.0 containing 0.1 M NaCl). Mg-ion chelate resin in PB (10 mM; pH 7.0 containing 0.1 M NaCl) (200 μ L) was added to the cell suspension to suppress enzymatic degradation of genomic DNA, and the resulting cell suspension was heated at 90 °C for 10 min to break the cells. After cooling to room temperature, RNase

inhibitor (20 μ L, 800 U) was added to the solution. The solution was centrifuged at 5600g for 10 min to remove the Mg-ion chelate resin and debris. The cell lysate (supernatant) was transferred to a fresh tube and stored at -20°C until use. The protein concentration of the cell lysate was determined to be 298 $\mu\text{g}/\text{mL}$ using the Bradford protein assay, in which a calibration curve was obtained using HSA. The CCLCR assay was carried out to detect target DNA and target RNA from human cell lysate. Specifically, 7 μL of target DNA (10 aM) or target RNA (10 aM) was added to 5 μL of the human cell lysate ($[\text{protein}] = 298 \mu\text{g}/\text{mL}$) prior to the assay. The resulting human cell lysate (12 μL) containing target DNA or target RNA was added to the assay mixture as described above. Final concentration of target DNA or target RNA was 1 aM. Thermal cycling conditions (denaturation at 85°C for 30 s and hybridization/ligation at 25°C for 150 s) and number of thermal cycles (40) were identical to those described previously for the CCLCR assay. The detection procedures were identical to those described previously for the CCLCR assay.

Conflict of Interest: The authors declare no competing financial interest.

Acknowledgment. This work was partially supported by a Grant-in-Aid for Scientific Research (C) (No. 24510165) from the Japan Society for the Promotion of Science (JSPS).

Supporting Information Available: Additional data as described in the text are available free of charge via the Internet at <http://pubs.acs.org>.

REFERENCES AND NOTES

- Kreibig, U.; Genzel, L. Optical Absorption of Small Metallic Particles. *Surf. Sci.* **1985**, *156*, 678–700.
- Ghosh, S. K.; Pal, T. Interparticle Coupling Effect on the Surface Plasmon Resonance of Gold Nanoparticles: From Theory to Applications. *Chem. Rev.* **2007**, *107*, 4797–4862.
- Murphy, C. J.; Gole, A. M.; Stone, J. W.; Sisco, P. N.; Alkilany, A. M.; Goldsmith, E. C.; Baxter, S. C. Gold Nanoparticles in Biology: Beyond Toxicity to Cellular Imaging. *Acc. Chem. Res.* **2008**, *41*, 1721–1730.
- Giljohann, D. A.; Seferos, D. S.; Daniel, W. L.; Massich, M. D.; Patel, P. C.; Mirkin, C. A. Gold Nanoparticles for Biology and Medicine. *Angew. Chem., Int. Ed.* **2010**, *49*, 3280–3294.
- Mirkin, C. A.; Letsinger, R. L.; Mucic, R. C.; Storhoff, J. J. A DNA-Based Method for Rationally Assembling Nanoparticles into Macroscopic Materials. *Nature* **1996**, *382*, 607–609.
- Elghanian, R.; Storhoff, J. J.; Mucic, R. C.; Letsinger, R. L.; Mirkin, C. A. Selective Colorimetric Detection of Polynucleotides Based on the Distance-Dependent Optical Properties of Gold Nanoparticles. *Science* **1997**, *277*, 1078–1081.
- Reynolds, R. A.; Mirkin, C. A.; Letsinger, R. L. Homogeneous, Nanoparticle-Based Quantitative Colorimetric Detection of Oligonucleotides. *J. Am. Chem. Soc.* **2000**, *122*, 3795–3796.
- Shen, W.; Deng, H.; Gao, Z. Gold Nanoparticle-Enabled Real-Time Ligation Chain Reaction for Ultrasensitive Detection of DNA. *J. Am. Chem. Soc.* **2012**, *134*, 14678–14681.
- Shen, W.; Deng, H.; Teo, A. K. L.; Gao, Z. Colorimetric Detection of Single-Nucleotide Polymorphisms with a Real-Time PCR-Like Sensitivity. *Chem. Commun.* **2012**, *48*, 10225–10227.
- Yin, H.; Huang, X.; Ma, W.; Xu, L.; Zhu, S.; Kuang, H.; Xu, C. Ligation Chain Reaction Based Gold Nanoparticle Assembly for Ultrasensitive DNA Detection. *Biosens. Bioelectron.* **2014**, *52*, 8–12.
- Storhoff, J. J.; Lazarides, A. A.; Mucic, R. C.; Mirkin, C. A.; Letsinger, R. L.; Schatz, G. C. What Controls the Optical Properties of DNA-Linked Gold Nanoparticle Assemblies? *J. Am. Chem. Soc.* **2000**, *122*, 4640–4650.
- Thanh, N. T. K.; Rosenzweig, Z. Development of an Aggregation-Based Immunoassay for Anti-Protein A Using Gold Nanoparticles. *Anal. Chem.* **2002**, *74*, 1624–1628.
- Kleppe, K.; van de Sande, J. H.; Khorana, H. G. Polynucleotide Ligase-Catalyzed Joining of Deoxyribo-Oligonucleotides on Ribopolynucleotide Templates and of Ribonucleotides on Deoxyribopolynucleotide Templates. *Proc. Natl. Acad. Sci. U.S.A.* **1970**, *67*, 68–73.
- Fareed, G. C.; Wilt, E. M.; Richardson, C. C. Enzymatic Breakage and Joining of Deoxyribonucleic Acid. VIII Hybrids of Ribo- and Deoxyribonucleotide Homopolymer as Substrates for Polynucleotide Ligase of Bacteriophage T4. *J. Biol. Chem.* **1971**, *246*, 925–932.
- Nilsson, M.; Barbany, G.; Antson, D.-O.; Gertow, K.; Landegren, U. Enhanced Detection and Distinction of RNA by Enzymatic Probe Ligation. *Nat. Biotechnol.* **2000**, *18*, 791–793.
- Shelbourne, M.; Chen, X.; Brown, T.; El-Sagheer, A. H. Fast Copper-Free Click DNA Ligation by the Ring-Strain Promoted Alkyne-Azide Cycloaddition Reaction. *Chem. Commun.* **2011**, *47*, 6257–6259.
- Heuer-Jungemann, A.; Kirkwood, R.; El-Sagheer, A. H.; Brown, T.; Kanaras, A. G. Copper-Free Click Chemistry as an Emerging Tool for the Programmed Ligation of DNA-Functionalised Gold Nanoparticles. *Nanoscale* **2013**, *5*, 7209–7212.
- Ning, X.; Guo, J.; Wolfert, M. A.; Boons, G.-J. Visualizing Metabolically Labeled Glycoconjugates of Living Cells by Copper-Free and Fast Huisgen Cycloadditions. *Angew. Chem., Int. Ed.* **2008**, *47*, 2253–2255.
- Laughlin, S. T.; Baskin, J. M.; Amacher, S. L.; Bertozzi, C. R. *In Vivo* Imaging of Membrane-Associated Glycans in Developing Zebrafish. *Science* **2008**, *320*, 664–667.
- Jewett, J. C.; Sletten, E. M.; Bertozzi, C. R. Rapid Cu-Free Click Chemistry with Readily Synthesized Biarylazacyclooctynes. *J. Am. Chem. Soc.* **2010**, *132*, 3688–3690.
- Oishi, M.; Nakao, S.; Kato, D. Enzyme-Free Fluorescent-Amplified Aptasensors Based on Target-Responsive DNA Strand Displacement via Toehold-Mediated Click Chemical Ligation. *Chem. Commun.* **2014**, *50*, 991–993.
- Storhoff, J. J.; Elghanian, R.; Mucic, R. C.; Mirkin, C. A.; Letsinger, R. L. One-Pot Colorimetric Differentiation of Polynucleotides with Single Base Imperfections Using Gold Nanoparticle Probes. *J. Am. Chem. Soc.* **1998**, *120*, 1959–1964.
- Demers, L. M.; Mirkin, C. A.; Mucic, R. C.; Reynolds, R. A.; Letsinger, R. L.; Elghanian, R.; Viswanadham, G. A Fluorescence-Based Method for Determining the Surface Coverage and Hybridization Efficiency of Thiol-Capped Oligonucleotides Bound to Gold Thin Films and Nanoparticles. *Anal. Chem.* **2000**, *72*, 5535–5541.
- Rosi, N. L.; Giljohann, D. A.; Thaxton, C. S.; Lytton-Jean, A. K. R.; Han, M. S.; Mirkin, C. A. Oligonucleotide-Modified Gold Nanoparticles for Intracellular Gene Regulation. *Science* **2006**, *312*, 1027–1030.
- Hurst, S. J.; Lytton-Jean, A. K. R.; Mirkin, C. A. Maximizing DNA Loading on a Range of Gold Nanoparticle Sizes. *Anal. Chem.* **2006**, *78*, 8313–8318.
- Rosi, N. L.; Mirkin, C. A. Nanostructures in Biodiagnostics. *Chem. Rev.* **2005**, *105*, 1547–1562.
- Barany, F. Genetic Disease Detection and DNA Amplification Using Cloned Thermostable Ligase. *Proc. Natl. Acad. Sci. U.S.A.* **1991**, *88*, 189–193.
- Claridge, S. A.; Mastrianni, A. J.; Au, Y. B.; Liang, H. W.; Micheal, C. M.; Fréchet, J. M. J.; Alivisatos, A. P. Enzymatic Ligation Creates Discrete Multinanoparticle Building Blocks for Self-Assembly. *J. Am. Chem. Soc.* **2008**, *130*, 9598–9605.
- Valentini, P.; Fiammengo, R.; Sabella, S.; Gariboldi, M.; Maiorano, G.; Cingolani, G.; Pompa, P. P. Gold-Nanoparticle-Based Colorimetric Discrimination of Cancer-Related Point Mutations with Picomolar Sensitivity. *ACS Nano* **2013**, *7*, 5530–5538.
- Halford, W. P. The Essential Prerequisites for Quantitative RT-PCR. *Nat. Biotechnol.* **1999**, *17*, 835.
- Schweitzer, B.; Kingsmore, S. Combining Nucleic Acid Amplification and Detection. *Curr. Opin. Biotechnol.* **2001**, *12*, 21–27.

32. Sutthent, R.; Gaudart, N.; Chokpaibulkit, K.; Tanliang, N.; Kanoksinsombath, C.; Chaisilwatana, P. p24 Antigen Detection Assay Modified with a Booster Step for Diagnosis and Monitoring of Human Immunodeficiency Virus Type 1 Infection. *J. Clin. Microbiol.* **2003**, *41*, 1016–1022.
33. Sidransky, D. Emerging Molecular Markers of Cancer. *Nat. Rev. Cancer* **2002**, *2*, 210–219.
34. Diehl, F.; Diaz, L. A., Jr. Digital Quantification of Mutant DNA in Cancer Patients. *Curr. Opin. Oncol.* **2007**, *19*, 36–42.
35. Modrich, P. DNA Mismatch Correction. *Annu. Rev. Biochem.* **1987**, *56*, 435–466.
36. Ross, J. S.; Linette, G. P.; Stec, J.; Ross, M. S.; Anwar, S.; Boguniewicz, A. DNA Ploidy and Cell Cycle Analysis in Breast Cancer. *Am. J. Clin. Pathol.* **2003**, *120*, S72–S84.
37. Tan, C. W.; Gardiner, B. S.; Hirokawa, Y.; Layton, M. J.; Smith, D. W.; Burgess, A. W. Wnt Signalling Pathway Parameters for Mammalian Cells. *PlosOne* **2012**, *7*, e31882.